Global atmospheric black carbon inferred from AERONET

Makiko Sato*†, James Hansen*†‡, Dorothy Koch*†, Andrew Lacis*†, Reto Ruedy*§, Oleg Dubovik¶, Brent Holben¶, Mian Chin¶, and Tica Novakov‖

*National Aeronautics and Space Administration Goddard Institute for Space Studies and †Columbia University Earth Institute, New York, NY 10025; §SGT, Inc., 2880 Broadway, New York, NY 10025; ¶Goddard Space Flight Center, Greenbelt, MD 20771; and ‖Lawrence Berkeley National Laboratory, Berkeley, CA 94720

Contributed by James Hansen, April 1, 2003

AERONET, a network of well calibrated sunphotometers, provides data on aerosol optical depth and absorption optical depth at >250 sites around the world. The spectral range of AERONET allows discrimination between constituents that absorb most strongly in the UV region, such as soil dust and organic carbon, and the more ubiquitously absorbing black carbon (BC). AERONET locations, primarily continental, are not representative of the global mean, but they can be used to calibrate global aerosol climatologies produced by tracer transport models. We find that the amount of BC in current climatologies must be increased by a factor of 2–4 to yield best agreement with AERONET, in the approximation in which BC is externally mixed with other aerosols. The inferred climate forcing by BC, regardless of whether it is internally or externally mixed, is ≈1 W/m², most of which is probably anthropogenic. This positive forcing (warming) by BC must substantially counterbalance cooling by anthropogenic reflective aerosols. Thus, especially if reflective aerosols such as sulfates are reduced, it is important to reduce BC to minimize global warming.

aerosols | air pollution | climate change

Global climate forcing by black carbon (BC) aerosols is uncertain in magnitude. The Intergovernmental Panel on Climate Change estimated a global mean BC forcing of 0.1 W/m² in their 1996 report (1), but in 2001 they raised this to 0.3 W/m² (2). Others (3, 4) suggest that the BC forcing is probably larger, ≈0.5 W/m² or more. The BC forcing needs to be known accurately for the sake of interpreting past climate change, projecting future change, and developing the most effective strategies for mitigating anthropogenic climate change.

It is difficult to determine the BC climate forcing by using emission estimates and aerosol transport models, because of imprecise knowledge of BC sources and uncertainties in simulation of aerosol removal mechanisms. We propose an alternative empirical approach for estimating the BC amount that uses photometer data in the long wave (red) portion of the spectrum. This approach is based on the fact that BC absorption exhibits a $1/\lambda$ spectral dependence over this entire wavelength range (5). This makes it possible to distinguish BC from other absorbing aerosols, specifically organic carbon (OC) and soil dust, which have appreciable absorption only at $\lambda < 600$ nm (6). We employ the optical depths for aerosol absorption (τ_a) measured by AERONET photometers (7, 8) at >250 sites around the world. We compare the aerosol absorption measured by AERONET with the aerosol absorption in two aerosol climatologies, which we label Koch (9) and Chin (10). This comparison yields a factor by which the BC climatologies must be altered to achieve best agreement with AERONET observations.

The aerosol compositions are treated as if they were externally mixed in the aerosol climatologies and in our radiative forcing calculations. This assumption does not affect our resulting estimate for the BC climate forcing, because both the forcing and the AERONET-measured τ_a depend on the BC absorption, not the BC mass. However, it means that, because internally mixed BC absorbs more effectively (3, 11), the BC mass may be less than obtained in the externally mixed approximation.

We first describe the AERONET data and the aerosol climatologies. We discuss assumed optical properties for soil dust and OC, because the absorption by these aerosols is not negligible in comparison with that of BC. We then estimate the amounts of BC and OC that provide the best match to aerosol absorption measured by AERONET. Finally we calculate the climate forcing associated with the inferred BC amount and discuss implications for strategies to minimize anthropogenic climate effects.

AERONET Data

AERONET is an internationally federated, globally distributed network of automatic sun and sky scanning radiometers that routinely observe and transmit observations for processing and posting to the AERONET web site (7). The instruments are returned annually to Goddard Space Flight Center in Greenbelt, MD, for calibration against Mauna Loa Langley calibrated reference instruments for aerosol optical depth (±0.01) and a National Institute of Standards and Technology referenced integrating sphere for sky radiances (>5% absolute accuracy). Our analysis uses the quality assured data that were available in late November of 2002, when there were 322 AERONET sites, of which 263 had data available for at least 1 month.

The processing method for the AERONET data (8, 12) involves fitting the multiangle multiwavelength observations with Mie scattering calculations, yielding best-fit values for aerosol (extinction) optical thickness (τ) and aerosol absorption optical thickness (τ_a). We employ the AERONET calculated monthly means of τ and τ_a. These data are available for four narrow wavelength bands centered at 440, 670, 870 and 1,020 nm.

We prepare the AERONET data for map display and comparison with aerosol model climatologies as follows. If there are two or more stations within a $1° \times 1°$ box for any given month, their data (for τ and τ_a) are combined with equal weights. Further, data for the $1° \times 1°$ boxes within each $4° \times 5°$ box are combined with equal weights. If there are at least 2 months with data in a given season for a given ($4° \times 5°$) grid box, we calculate the seasonal means of τ and τ_a. The number of $4° \times 5°$ boxes with seasonal mean data are thus 102 (March–April–May), 117 (June–July–August), 108 (September–October–November), and 81 (December–January–February). Annual means are calculated for the 95 $4° \times 5°$ boxes with at least three seasons of data.

There are 3,312 $4° \times 5°$ grid boxes on the globe, so the 95 boxes with annual data cover ≈3% of the world. The locations of the boxes with data are shown in later figures in this paper. Coverage is good in the United States, Europe, and most of South America and Southern Africa.

We do not imply that a single station should be taken as providing a representative mean for a $4° \times 5°$ region. One can

Abbreviations: BC, black carbon; OC, organic carbon.

‡To whom correspondence should be addressed. E-mail: jhansen@giss.nasa.gov.

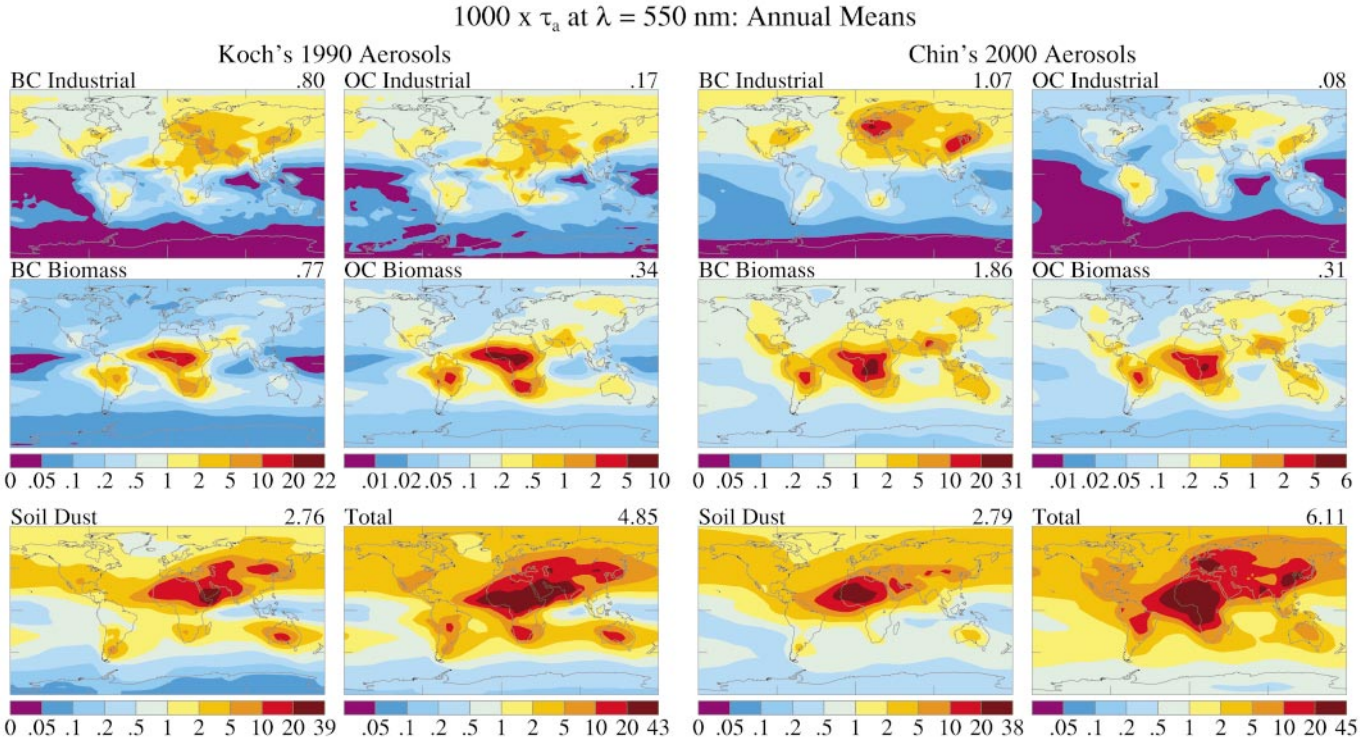

Fig. 1. Aerosol absorption (1,000 × τ_a) at λ = 550 nm based on the chemical transport models of Koch (*Left*) and Chin (*Right*).

argue that, because of the small-scale heterogeneity of aerosols, many stations are required within a 4° × 5° box to obtain grid box mean values. On the other hand, the atmospheric lifetime of aerosols is typically several days, during which time the aerosols can travel thousands of kilometers, even though the aerosols may undergo physical and chemical changes during that period. Thus, one way to estimate global aerosol distributions and global mean aerosol properties is to use observations such as those of AERONET to test and constrain the aerosol climatologies from aerosol chemical transport models. That is the essence of the approach that we employ in this study. Improvements in this approach will be possible in the future, as aerosol sources for the transport models are specified with more precision, transport calculations improve, and aerosol observations attain better coverage and include additional aerosol microphysical composition-related information.

Transport Model Climatologies

We employ aerosol climatologies from two chemical transport models, Koch and Chin, to obtain an indication of how the results depend on the assumed aerosol climatology. We use the same aerosol optical constants and size distributions in the two models to eliminate that as a source of difference between the two models. However, we vary aerosol optical constants and sizes to examine their influence on the results.

The Koch and Chin aerosol distributions differ because of differing sources, transports, and removal mechanisms. For the constituents of special interest here, global sources for Koch/Chin in Tg of C per year are 5.2/6.5 industrial BC, 6/11 biomass BC, 20.8/10.5 industrial OC, 47/77 biomass OC, and 8.7/12.7 terpene OC. "Industrial" refers to the total fossil fuel contribution, including transportation.

Fig. 1 compares τ_a in the Koch and Chin climatologies at wavelength λ = 550 nm (approximate midpoint of 440- and 670-nm AERONET channels). τ is provided in Fig. 7, which is published as supporting information on the PNAS web site, www.pnas.org. We also use the Chin sea salt distribution for Koch, because at the time of our computations Koch had not used her transport model to simulate sea salt. Koch's soil dust distribution is from an earlier study (13).

The global mean aerosol optical depth at 550 nm is 0.11 for Koch and 0.12 for Chin. Regional and species differences are larger. Chin has ≈50% more sulfate than Koch. Koch's industrial OC is about twice that of Chin, whereas Chin's biomass BC is two and one-half times greater than Koch's. These differences are indicative of large uncertainties in sources, models, and resulting aerosol amounts. Our objective is to derive information on global BC amount despite current uncertainties in aerosol distributions.

Aerosol Optical Properties

BC is believed to be the aerosol most responsible for absorption of solar radiation (14). However, OC (15) and soil dust (6) are also significant absorbers, especially in the UV region. Therefore, we need to account for the absorption of these latter aerosols as well as possible, before attempting to infer BC absorption from AERONET observations. In this section we define the optical properties that we used for all aerosols.

BC optical properties (16) have n_r varying from 1.56 to 1.60 and n_i from 0.48 to 0.53 over the relevant (AERONET) wavelength range. Sea salt is assumed to have n_r = 1.45 and n_i = 0 (16). Soil dust optical properties (17) have n_r varying from 1.6 to 1.54 and n_i varying from 0.024 to 0.005 over the relevant wavelengths. Sulfate is practically nonabsorbing at relevant wavelengths (18).

OC absorption properties are based on laboratory measurements on urban and biomass smoke samples at Lawrence Berkeley National Laboratory (T. Novakov, personal communication), which yield an OC absorption coefficient (m^2/g) of 2.75, 0.95, 0.42, 0.32, and 0.21 at λ = 400, 500, 600, 700, and 900 nm, respectively. The resulting values for $n_i = \lambda\rho\sigma_{abs}/4\pi$ are 0.029, 0.013, 0.007, 0.006, and 0.005 at the respective wavelengths. We assume that n_r = 1.5. The organic matter (OM) in

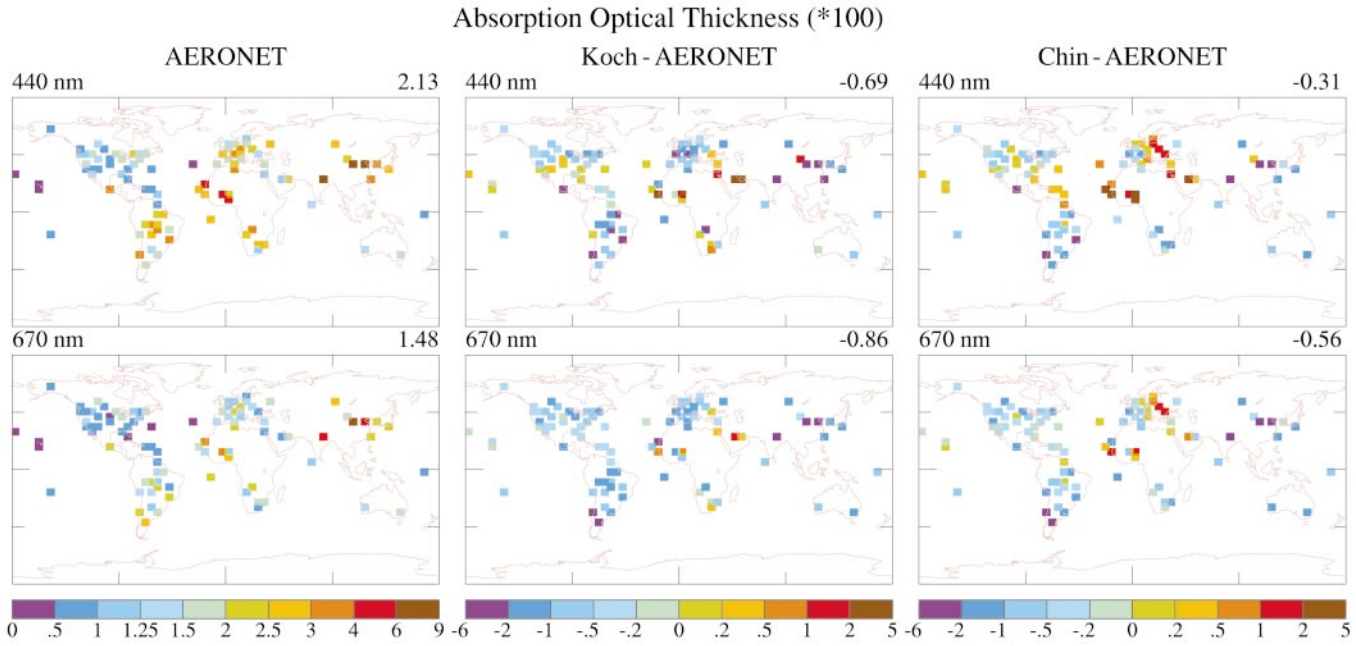

Fig. 2. Comparison of τ_a from Koch and Chin models with AERONET observations at 440 and 670 nm.

the tracer transport model is assumed to be OM = 1.5 OC, the additional portion of OM being nonabsorbing.

The calculated aerosol absorption and single scattering albedo (ω) also depend on the aerosol size distributions. However, we find that the inferred BC climate forcing is not sensitive to variations of the size distribution within reasonable ranges. Our calculations here use the gamma size distribution (19) with $v_{eff} = 0.2$. Most of our illustrations in this paper are for $r_{eff} = 0.2$ μm for BC, OC, and sulfate. The soil dust size distribution is defined elsewhere (13) and sea salt has $r_{eff} = 2$ μm. Use of the same r_{eff} for BC, OC, and sulfate might be appropriate if they are internally mixed. However, we also carried out our entire analysis with $r_{eff} = 0.04$ and 0.1 μm for BC and $r_{eff} = 0.3$ μm for OC and sulfate, for the purpose of verifying that our conclusions about the derived optical depth and climate forcing by BC were not affected by the aerosol size distribution. It is not surprising that the inferred spectrally integrated BC absorption is rather insensitive to the aerosol size distribution, because the AERONET wavelengths constraining the BC absorption are in the spectral region of maximum solar irradiance. Errors in the size distribution primarily affect the calculated absorption at wavelengths outside the AERONET range.

Comparisons with AERONET Data

Fig. 2 compares τ_a observed by AERONET with τ_a calculated by using the aerosol climatologies (models) of Koch and Chin. The wavelengths illustrated, 440 and 670 nm, are the AERONET wavelengths closest to $\lambda = 550$ nm, where aerosol climatologies are usually defined. The numbers in the upper-right corners are area-weighted "global" means for grid boxes with data, so they are biased toward the large values that occur over land.

It is apparent that both models, especially Koch's, underestimate τ_a at most AERONET locations. Primary exceptions are a few grid-boxes in northern Africa, where both models have more absorption than observed, and in Europe, where Chin has more absorption than observed by AERONET.

Soil Dust. Excess absorption occurs in northern Africa in the models despite the fact that aerosol optical depth (Fig. 7) in the models is less than observed there. This finding suggests that the soil dust absorption coefficient is too large in that region. Others (8, 20, 21) have noted that the desert dust in this region is much less absorbing than is obtained with the soil dust properties that we have used (17).

It is desirable to minimize errors in the models' soil dust

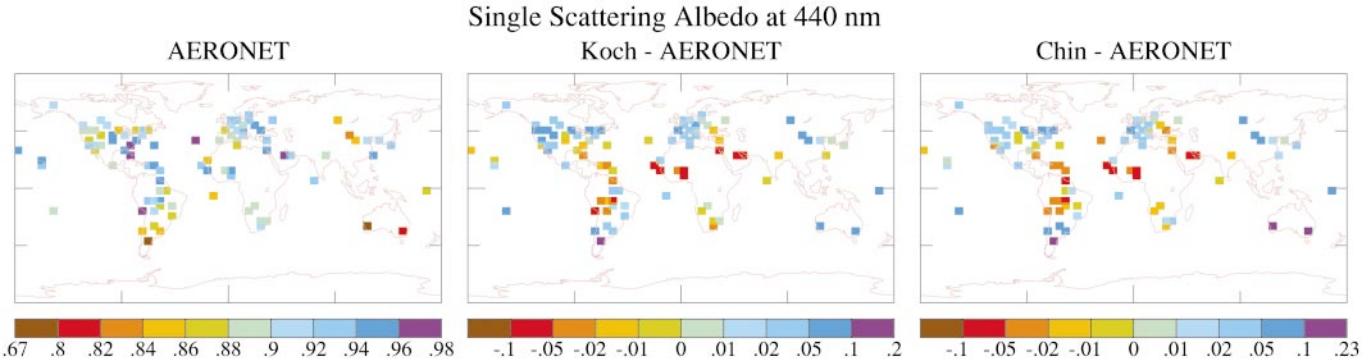

Fig. 3. Comparison of ω from Koch and Chin models, using aerosol optical properties described in our text, with AERONET observations for the "full" soil dust absorption coefficient of Patterson *et al.* (17).

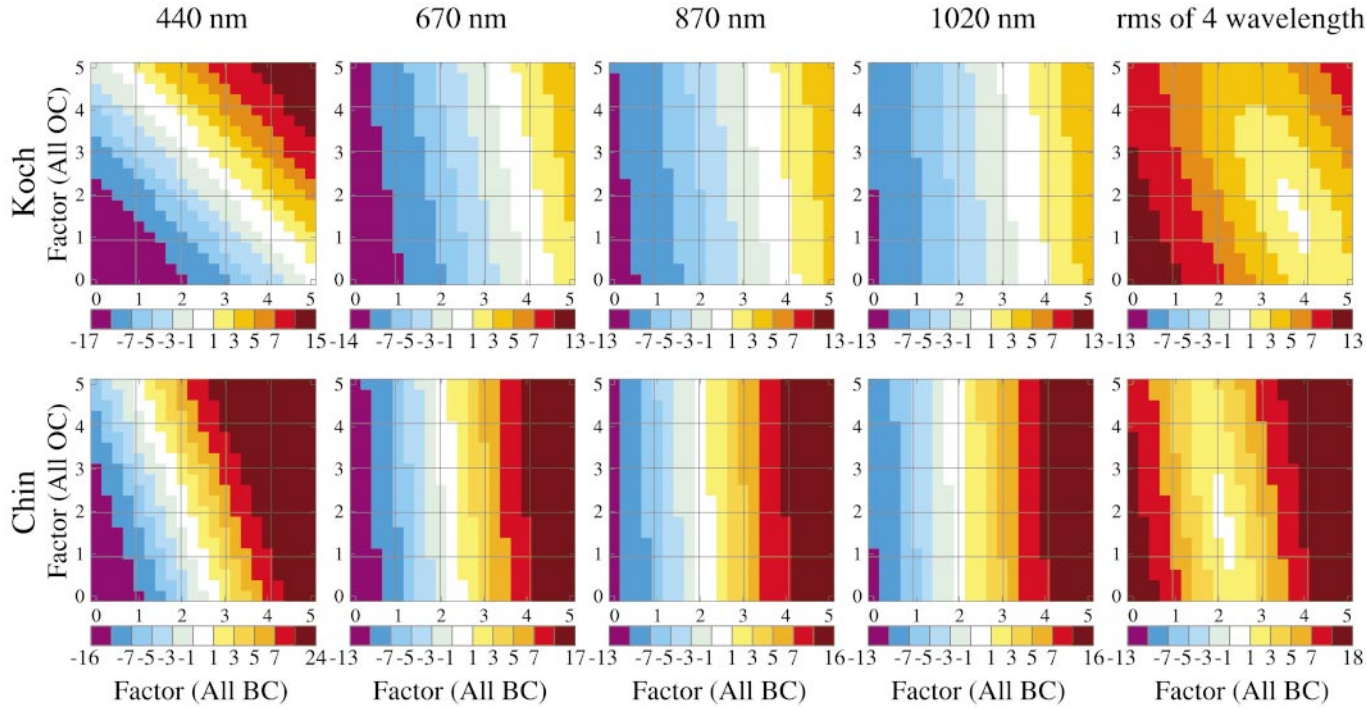

Fig. 4. Difference between modeled and AERONET-measured τ_a, averaged over grid boxes with AERONET stations, as a function of the factors by which the models' BC and OC amounts are multiplied. The fifth column is the rms for the four AERONET wavelengths.

absorption before using the models for inferences about absorption by BC. The soil dust effect can be seen clearly in ω at the shortest wavelength, 440 nm, shown in Fig. 3. Even when the soil dust absorption coefficient is reduced by one-half, the calculated absorption is excessive in several grid boxes in northern Africa. However, soil dust absorption varies considerably from one place in the world to another, with the Sahara being a relatively high albedo desert (6). Thus, a single soil dust absorption coefficient cannot yield good agreement with observed absorption everywhere. We take, for our standard case, the reduced (50%) soil dust absorption coefficient. However, we also carry out calculations with the larger soil dust absorption coefficient to show that the uncertainty in soil dust absorption has only a minor impact on the inferred BC absorption.

BC and OC. The other known absorbing aerosols, in addition to soil dust, are BC and OC. BC is the primary absorber at the three longer AERONET wavelengths, as mentioned above. However, because there is uncertainty about the global amounts of both BC and OC, we wish to allow both BC and OC to be variables as we try to find a best fit with AERONET observations. Because Koch and Chin assume a different ratio of BC/OC emissions (see above), it is of interest to see whether the AERONET analysis can constrain this ratio.

Fig. 4 shows the difference between model τ_a and AERONET-measured τ_a ("global" means) as a function of the factors, F_{BC} and F_{OC}, by which BC and OC amounts are changed individually in the models. At a given wavelength, any combination of BC and OC amounts within the white region provides a good fit to the observed τ_a. However, the rms best fit for the combination of all wavelengths, shown in the fifth column of Fig. 4, yields a reasonably well defined set of F_{BC} and F_{OC} for each of the Koch and Chin climatologies. The factors are different for Koch and Chin, but after multiplication by the amounts of BC and OC in their unmodified climatologies, we find similar amounts for both BC and OC (Table 1).

The consistency of the derived BC and OC amounts between the Koch and Chin distributions, despite their large differences in aerosol sources and distributions, provides one piece of evidence that the required very large increase in BC (factor of ≈2–4) and large increase in OC (factor of ≈1.5–2) are meaningful. In addition, the results are consistent at all three of the longer wavelengths (Fig. 4), where BC is the primary absorber.

BC and OC sources are uncertain, and the ratio of their source strengths is different in the Koch and Chin climatologies. However, this difference between Koch and Chin is largely removed when we allow BC and OC to vary independently in fitting to AERONET data (Table 1). The resulting global BC/OC ratio is about twice as large as in the estimated sources. Thus we speculate that, rather than the BC/OC source ratio being that much in error, the result is an indication that most BC is internally mixed, as discussed below.

Discussion

Our conclusion, that there is more atmospheric absorption by BC aerosols than has generally been realized, seems difficult to deny unless one argues either that AERONET measurements are inaccurate, with excessively large absorption, or that there is

Table 1. τ and τ_a at 550 nm for BC and OC in original and modified climatologies

		Koch		Chin	
		τ	τ_a	τ	τ_a
Original Climatology	BC	0.003	0.0016	0.005	0.0029
	OC	0.016	0.0005	0.012	0.0004
Multiplying Factor	BC	3.8	3.8	2.2	2.2
	OC	1.6	1.6	1.8	1.8
Inferred Amount	BC	0.010	0.0060	0.011	0.0064
	OC	0.025	0.0008	0.022	0.0007

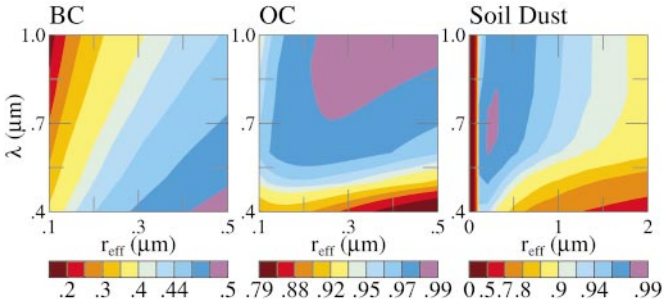

Fig. 5. Single scattering albedo ω (r_{eff}, λ) for BC, OC, and soil dust aerosols.

another strong absorber at the red wavelengths, in addition to BC. We comment here on both of these possibilities.

Aerosol absorption is summarized in the single scatter albedo, ω. The AERONET sites, mostly continental, have mean ω that decreases monotonically from 0.914 at 670 nm to 0.897 at 1,020 nm. There are several dozen papers reporting measurements of aerosol absorption at various places around the world in recent decades. These results provide no general indication that AERONET is overstating aerosol absorption. Based on such comparisons and on validations of the AERONET measurements (7, 8, 22), there is no indication that AERONET is exaggerating aerosol absorption.

If there is an unidentified material providing the absorption, the absorber would need to have properties similar to those of BC in the sense of providing comparable absorption at all three AERONET channels between 670 and 1,020 nm. Although there have been suggestions of a possible mystery atmospheric absorber (23, 24), it has been shown that aerosols and water vapor accurately reproduce atmospheric transmission data (25). Also, AERONET measurements indicate that there is no significant nonaerosol absorption in spectral bands without gaseous absorption (26), and it has been shown (ref. 27 and references therein) that BC accounts for most of the aerosol absorption in continental regions.

Fig. 5, which shows ω (r_{eff}, λ) for BC, OC, and soil dust, clarifies why BC can match the absorption measured by AERONET and the other aerosols cannot. AERONET retrievals show that the aerosols become slightly darker as λ increases from 670 to 1,020 nm. Fig. 5*a* shows that BC becomes gradually darker toward longer λ, so that, when combined with the predominant nonabsorbing aerosols, it is easy to achieve a rather flat ω, decreasing slightly to longer wavelengths. OC and soil dust have the opposite behavior for any reasonable particle size. Although one can hypothesize an unidentified absorber, Occam's razor favors BC as the primary absorber at the red wavelengths.

Climate Forcing. Fig. 6 shows the BC climate forcing calculated for the BC amount that we inferred from the Koch and Chin models, the global means being 0.91 and 1.05 W/m^2. OC forcings for Koch and Chin are -0.45 and -0.38 W/m^2, with most of this forcing from biomass burning, but OC forcings are poorly constrained by AERONET because of the similarity of OC and soil dust absorption spectra. These forcings are calculated with the assumption that aerosol optical depths are similar in clear and cloudy regions, an assumption that may exaggerate the climate forcings, because the rainout preferentially reduces aerosols in cloudy regions. Because rain occurs in only a fraction of the cloudy area and does not scavenge 100% of the aerosols, and because aerosols occur above and below the clouds, it seems unlikely that the average aerosol burden in cloudy regions is reduced by more than half.

The fossil fuel portion of the BC climate forcing (35% for Chin and 50% for Koch, but our analysis provided no check on these proportions) must be anthropogenic, and part of the biomass/biofuels BC is natural. Thus, accounting also for reduced aerosol amount in cloudy regions, we estimate the anthropogenic BC forcing as $\approx 0.7 \pm 0.2$ W/m^2. The indicated uncertainty is a subjective 1σ error estimate.

This BC climate forcing is larger than the 0.3 W/m^2 estimated by the Intergovernmental Panel on Climate Change (2001), although we note that this estimate referred only to the fossil fuel component. The derived BC climate forcing is reasonably consistent with an estimate (3) of ≈ 0.5 W/m^2 for the fossil fuel component. It is also consistent with the estimate 0.8 ± 0.4 W/m^2 for the total BC forcing (4) that included indirect BC forcings such as reduced snow albedo.

Internal vs. External Mixing. The mass of BC implied by our results is 2.0 ± 0.4 mg/m^2 (or 1.0 Tg globally), assuming that the BC occurs as externally mixed particles with $r_{eff} = 0.2$ μm. Much of the BC may in reality be combined with other constituents. Absorption by BC specks that adhere to the outside of other particles is accurately rendered by the externally mixed approximation (M. Mishchenko, personal communication). However, if the BC is internally mixed, as it is with sulfate coating on BC, the absorption effectiveness is altered. Specifically, it has been shown that the average of all possible locations of BC within a sulfate particle is accurately represented by the Bruggeman or Maxwell-Garnett effective medium approximation (11). In that case absorption by BC within sulfate aerosols is a factor of 2–2.5 greater than by BC in free air (i.e., BC externally mixed). Thus, if internal mixing is the more common situation, the actual mass of BC may be only about half of that estimated from the externally mixed approximation, i.e., ≈ 1 mg/m^2. Reality presumably lies somewhere between these two situations, but we suggest that it may be closer to the internally mixed case for the

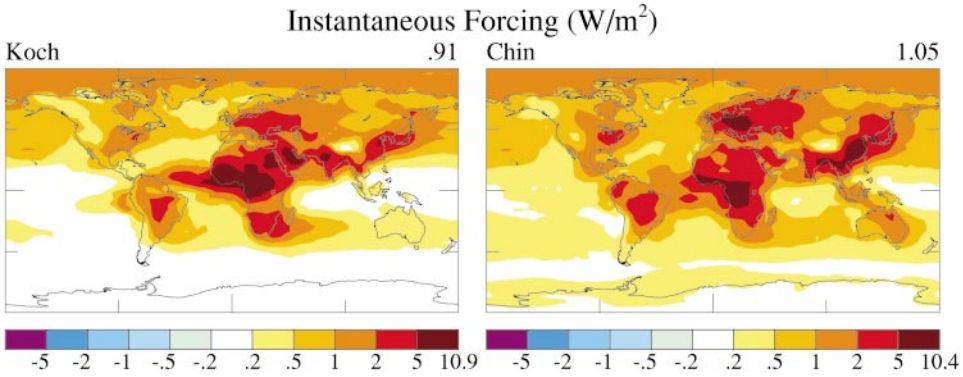

Fig. 6. Climate forcing by BC based on the Koch and Chin models modified by AERONET.

reason given in the final section above. The global atmospheric mass of BC is thus in the range 0.5–1.0 Tg, but probably closer to the lower value.

Practical Implications. We conclude that BC aerosols cause a larger climate forcing than has been assumed by the Intergovernmental Panel on Climate Change (1, 2). This large positive climate forcing has occurred in approximately the same regions of the globe as the negative direct and indirect climate forcings by reflective aerosols (sulfates, nitrates, and OC). We suggest that this large positive BC forcing provides a partial explanation for why global warming has proceeded rapidly despite the fact that the estimated negative (direct plus indirect) forcing by reflective aerosols is almost as large as the positive forcing by long-lived greenhouse gases (2, 4). Another air pollutant, tropospheric ozone, contributes in a similar way to BC (4).

If, as we suggest, BC has substantially reduced the net cooling effect of anthropogenic aerosols, there is a danger that policies designed to reduce reflective aerosols, such as sulfates and nitrates that cause acid rain, could accelerate global warming. This suggests that policy-makers should place at least as much emphasis on reducing BC aerosols ("soot") as on reducing reflective aerosols.

Jacobson (3) goes even further, suggesting that reducing BC aerosols may be the best strategy to slow global warming, perhaps more effective than slowing CO_2 emissions. That is unlikely. Reduction of BC emissions could minimize the global warming bounce that will result from reductions in reflective aerosols, but, at best, the net cooling effect will be small, for several reasons. First, actions to reduce BC will also reduce OC from the same sources, and, as shown above, the negative OC forcing counterbalances about half of the BC forcing. Second, some of the actions that reduce BC and OC require reducing the sulfur content of fuels, which will reduce the negative forcing by sulfate aerosols. Third, reduced aerosol amounts will tend to reduce the (negative) indirect aerosol forcing because of their effects on clouds (2). Fourth, the efficacy of the direct climate forcing by absorbing aerosols is less than that for the same forcing by CO_2 and other well mixed greenhouse gases, i.e., it is less effective in producing warming of surface air temperature (28). For these reasons, the cooling effect of actions to reduce BC emissions will be small. Nevertheless, we agree that such actions are desirable not only to minimize the warming from expected reductions in reflective aerosols, but also to reduce the regional climate impacts of BC aerosols (29) and the human health and agricultural impacts of these aerosols.

Despite the uncertainties in the several climate forcings associated with actions designed to reduce aerosols, meaningful implications can be drawn for both developing and developed countries. The large emissions of soot aerosols in developing countries have negative impacts on human health, agricultural productivity, regional climate, and global warming. Reductions of soot emissions from cook-stoves, polluting industries, and vehicles thus would have multiple benefits.

In developed countries, diesel-powered vehicles are one of the largest sources of BC aerosols. Although there are plans to reduce such emissions from trucks, buses, and off-road vehicles in many developed countries, there is also a trend toward increasing use of diesel automobiles. This latter trend is driven by the higher efficiency of diesel engines, and thus reduced fuel cost and reduced CO_2 emissions. However, diesel engines produce much more BC, and although particle traps can capture most of the BC, these traps are expensive and it may be difficult to assure use of the traps for the life of the vehicle. Gasoline–electric hybrid engines are a diesel alternative that reduce both CO_2 and BC emissions, thus presenting a win–win option for climate and human health.

We thank Tsengdar Lee and Don Anderson, managers of the National Aeronautics and Space Administration Climate Modeling and Atmospheric Radiation programs, respectively, for their support of our research, David Giles and Ilya Slutsker for preparation of the AERONET data for our analysis, all of the AERONET participants who have contributed to the global database, Greg Carmichael for a helpful review of the paper, and Darnell Cain for technical assistance.

1. Intergovernmental Panel on Climate Change (1996) *Climate Change 1995: The Science of Climate Change*, eds. Houghton, J. T., Meira, L. G., Callander, B. A., Harris, N., Kattenberg, A. & Maskell, K. (Cambridge Univ. Press, Cambridge, U.K.).
2. Intergovernmental Panel on Climate Change (2001) *Climate Change 2001: The Scientific Basis*, eds. Houghton, J. T., Ding, Y., Griggs, D. J., Noguer, M., van der Linden, P. J., Dai, X., Maskell, K. & Johnson, C. A. (Cambridge Univ. Press, Cambridge, U.K.).
3. Jacobson, M. Z. (2001) *Nature* **409,** 695–697.
4. Hansen, J. E. & Sato, M. (2001) *Proc. Natl. Acad. Sci. USA* **98,** 14778–14783.
5. Bergstrom, R. W., Russell, P. B. & Hignett, P. (2002) *J. Atmos. Sci.* **59,** 567–577.
6. D'Almeida, G. A. (1987) *J. Geophys. Res.* **92,** 3017–3026.
7. Holben, B. N., Tanre, D., Smirnov, A., Eck, T. F., Slutsker, I., Abuhassan, N., Newcomb, W. W., Schafer, J., Chatenet, B., Lavenue, F., *et al.* (2001) *J. Geophys. Res.* **106,** 12067–12098.
8. Dubovik, O., Holben, B. N., Eck, T. F., Smirnov, A., Kaufman, Y. J., King, M. D., Tanre, D. & Slutsker, I. (2002) *J. Atmos. Sci.* **59,** 590–608.
9. Koch, D. (2001) *J. Geophys. Res.* **106,** 20311–20332.
10. Chin, M., Ginoux, P., Kinne, S., Torres, O., Holben, B. N., Duncan, B. N., Martin, R. V., Logan, J. A., Higurashi, A. & Nakajima, T. (2002) *J. Atmos. Sci.* **59,** 461–483.
11. Chylek, P., Videen, G., Ngo, D., Pinnick, R. G. & Klett, J. D. (1995) *J. Geophys. Res.* **100,** 16325–16322.
12. Dubovik, O. & King, M. D. (2000) *J. Geophys. Res.* **105,** 20673–20696.
13. Tegen, I. & Lacis, A. A. (1996) *J. Geophys. Res.* **101,** 19237–19244.
14. Horvath, H. (1993) *Atmos. Environ.* **27A,** 293–317.
15. Krivacsy, Z., Hoffer, A., Sarvari, Z., Temesi, D., Baltensperger, U., Nyeki, U., Weingartner, E., Kleefeld, S. & Jennings, S. G. (2001) *Atmos. Environ.* **35,** 6231–6244.
16. Nilsson, B. (1979) *Appl. Opt.* **18,** 3457–3473.
17. Patterson, E. M., Gillette, D. A. & Stockton, B. H. (1977) *J. Geophys. Res.* **82,** 3153–3160.
18. Toon, O. B., Pollack, J. B. & Khare, B. N. (1976) *J. Geophys. Res.* **81,** 5733–5748.
19. Hansen, J. E. & Travis, L. D. (1974) *Space Sci. Rev.* **16,** 527–610.
20. Kaufman, Y. J., Tanre, D., Dubovik, O., Karnieli, A. & Remer, L. A. (2001) *Geophys. Res. Lett.* **28,** 1479–1482.
21. Takemura, T., Nakajima, T., Dubovik, O., Holben, B. N. & Kinne, S. (2002) *J. Clim.* **15,** 333–352.
22. Haywood, J. M., Francis, P., Dubovik, O., Glew, M. & Holben, B. (2003) *J. Geophys. Res.* **108(D13),** 8471, 10.1029/2002JD002250.
23. Cess, R. D., Zhang, M. H., Minnis, P., Corsetti, L., Dutton, E. G., Forgan, B. W., Garber, P., Gates, W. L., Hack, J. J., Harrison, E. F., *et al.* (1995) *Science* **267,** 496–499.
24. Ramanathan, V., Subasilar, B., Zhang, G. J., Conant, W., Cess, R. D., Kiel, J. T., Grassl, H. & Shi, L. (1995) *Science* **267,** 499–503.
25. Hansen, J., Ruedy, R., Lacis, A., Sato, M., Nazarenko, L., Tausnev, N., Tegen, I. & Koch, D. (2000) in *General Circulation Model Development*, ed. Randall, D. (Academic, New York), pp. 127–164.
26. Kaufman, Y. J., Dubovik, O., Smirnov, A. & Holben, B. N. (2002) *Geophys. Res. Lett.* **29(18),** 1857, 10.1029/2001GL014399.
27. Huffman, H. D. (1996) *Atmos. Environ.* **30,** 73–83.
28. Hansen, J., Sato, M. & Ruedy, R. (1997) *J. Geophys. Res.* **102,** 6831–6864.
29. Menon, S., Hansen, J., Nazarenko, L. & Luo, Y. (2002) *Science* **297,** 2250–2253.